4

TECHNICAL MEMORANDUM

ANL-OTEC-78-1
Distribution Category UC-64

AN ANALYSIS OF HEAT TRANSFER IN HORIZONTAL TUBE FALLING FILM EVAPORATORS

by

J. J. Lorenz and D. Yung

Components Technology Division

Argonne National Laboratory

USDOE Division of Solar Technology

March 1978

DISCLAIMER

The facilities of Argonne National Laboratory are owned by the United States Government. Under the terms of a contract (W-31-109-Eng-38) between the U. S. Department of Energy, Argonne Universities Association and The University of Chicago, the University employs the staff and operates the Laboratory in accordance with policies and programs formulated, approved and reviewed by the Association.

MEMBERS OF ARGONNE UNIVERSITIES ASSOCIATION

The University of Arizona
Carnegie-Mellon University
Case Western Reserve University
The University of Chicago
University of Cincinnati
Illinois Institute of Technology
University of Illinois
Indiana University
Iowa State University
The University of Iowa
Kansas State University
The University of Kansas
Loyola University
Marquette University
Michigan State University
The University of Michigan
University of Minnesota
University of Missouri
Northwestern University
University of Notre Dame
The Ohio State University
Ohio University
The Pennsylvania State University
Purdue University
Saint Louis University
Southern Illinois University
The University of Texas at Austin
Washington University
Wayne State University
The University of Wisconsin

TECHNICAL MEMORANDUM

ANL-OTEC-78-1
Distribution Category UC-64

AN ANALYSIS OF HEAT TRANSFER IN HORIZONTAL TUBE FALLING FILM EVAPORATORS

by

J. J. Lorenz and D. Yung

Components Technology Division

Argonne National Laboratory

USDOE Division of Solar Technology

March 1978

Table of Contents

List of Figures

Nomenclature

C_p	specific heat
C_{sf}	constant in Rohsenow correlation, eq. (8a)
d	tube diameter
g	gravitational acceleration
$\bar{h}$	average heat transfer coefficient over L
h_b	boiling heat transfer coefficient
h_c	fully developed heat transfer coefficient, eqs. (8d) and (8e)
h_d	heat transfer coefficient in developing region
h_{fg}	latent heat of vaporization
k	thermal conductivity
L	circumferential length of heated surface
L_d	developing length, eq. (8c)
Pr	Prandtl number, $c\mu/k$
Re	Reynolds number, $4\Gamma/\mu$
t_d	diffusion time, eq. (1)
T_s	saturation temperature
T_w	wall temperature
ΔT	superheat $T_w - T_s$
U	overall coefficient of heat transfer
Z	vertical coordinate measured from top of tube
α	diffusivity of heat
Γ	flowrate per unit axial length of tube
δ	film thickness
μ	absolute viscosity
ν	kinematic viscosity
ρ	density
σ	surface tension

Abstract

A model of combined boiling and evaporation of liquid films on horizontal tubes was developed. Specifically, this work was directed toward developing a heat transfer model applicable to the design of horizontal tube falling film evaporators for OTEC. The heat transfer process is modelled as combined boiling and evaporation of the liquid film. In modelling the behavior of single tubes special account is taken of heat transfer in the initial thermal developing region of the film.

Predictions were found to agree favorably with the published experimental data of Fletcher et al. [1,2] for boiling and evaporation of thin water films on single horizontal tubes. The predicted upper and lower limits of heat transfer for ammonia on a vertical bank of plain horizontal tubes are 5.4 kW/m^2-K and 3.1 kW/m^2-K, respectively. The upper limit will be approached when the influence of between-tube evaporation and turbulence created by the liquid falling from one tube to the next are important. For an OTEC evaporator with plain tubes, the upper and lower limits of the overall U are 2.33 kW/m^2-K and 1.82 kW/m^2-K, respectively. With ammonia-side boiling enhancement, the overall U can be increased to about 3.8 kW/m^2-K.

1.0 Introduction

Relatively high heat fluxes can be achieved with small temperature differences by combined boiling and evaporation of thin liquid films on horizontal tubes. Evaporators employing these heat transfer mechanisms have been used in refrigeration systems, desalination plants, and, more recently, have been proposed for use in Ocean Thermal Energy Conversion (OTEC) power plants. A design of particular interest for OTEC is the horizontal tube falling film evaporator. This is a shell and tube unit with warm sea water on the tube side and working fluid (e.g., ammonia) on the shell side. Working fluid is supplied by feed tubes over vertical banks of horizontal tubes on which vaporization occurs. The upper portion of a typical tube bank comprising an evaporator unit is illustrated in Figure 1. Unevaporated fluid from any given tube falls on the next lower tube. Unevaporated liquid collects at the bottom of the evaporator and is recirculated. A major design challenge is to keep the tubes wetted (to ensure good heat transfer) with minimum recirculation (to minimize parasitic pumping).

Despite the importance of boiling and evaporation of liquid films on horizontal tubes, surprisingly little analytical and experimental work has appeared in the literature, e.g. [1-5]. Much of the previous work was sponsored by the Office of Saline Water (OSW) and was directed toward desalination. The present study is directed toward developing a heat transfer model which can be applied to the design of horizontal tube falling film evaporators for OTEC. Combined boiling and evaporation will be considered. Special account will be taken of heat transfer in the initial thermal developing region of the film. Predictions will be compared with published experimental data for evaporating water films on horizontal tubes. The model will be applied to ammonia and heat transfer coefficients will be predicted for vertical banks of plain and enhanced tubes. Limits of heat transfer performance will be established for horizontal tube falling film evaporators without water side enhancement.

2.0 Analysis

For the case of a single horizontal tube with outer diameter d, the problem is treated by "unwrapping" the tube to form a vertical surface of length $L = \pi\, d/2$, see Figure 2. Within the length L, two distinct convective heat transfer regions are defined: a thermal developing region and a fully developed region. If the superheat is sufficiently high, nucleate boiling can occur in the film. The overall heat transfer is modelled as a superposition of the convective components and the boiling component. In the following sub-sections, models of each heat transfer mechanism will be presented and then incorporated into an overall heat transfer model for single tubes. In addition controlling mechanisms of heat transfer for a vertical bank of horizontal tubes will be discussed. The influence of vapor crossflow is neglected in the present analysis. A detailed study of possible liquid redistribution and entrainment resulting from vapor crossflow is presently under investigation by the authors.

2.1 Thermal Developing Region

Referring to Figure 2, liquid at the saturation temperature T_s is fed at a flowrate 2Γ to the top of a heated tube, establishing a thin film on the surface. The feed flow splits evenly with Γ going to each side. A thermal developing length L_d is required for the film to be superheated from the saturation temperature to a fully developed linear profile. To an observer moving with the average film velocity, $\Gamma/\rho\delta$, the developing temperature profile is shown in Figure 3. The diffusion time t_d required for the temperature front to reach the interface is approximated as:

$$t_d = \frac{\delta^2}{4\pi\alpha} \tag{1}$$

This approximation is based on a consideration of 1-D transient heat conduction in a solid initially at uniform temperature and then subjected to a sudden step increase in temperature at a boundary. The film thickness δ is estimated from the well-known Nusselt expression:

$$\delta = \sqrt[3]{\frac{3\mu\Gamma}{g\rho^2}} \tag{2}$$

Multiplying the average film velocity by the diffusion time, the developing length is calculated to be:

$$L_d = \frac{\Gamma^{4/3}}{4\pi\rho\alpha}\sqrt[3]{\frac{3\mu}{g\rho^2}} \tag{3}$$

In the thermal developing region all the heat transferred from the wall goes into superheating the liquid film and no evaporation occurs. From an energy balance in the developing region, the total heat transfer per unit depth is $\frac{3}{8}\Gamma C_p \Delta T$. For this calculation a parabolic velocity profile and linear temperature profile were assumed at $Z = L_d$. The average heat transfer coefficient in the thermal developing region is then:

$$h_d = \frac{3}{8} C_p \frac{\Gamma}{L_d} \tag{4}$$

The heat transfer coefficient in the thermal developing region will generally be higher than that in the fully developed region. This is analogous to the case of single phase convective heat transfer in pipes where the heat transfer coefficient is substantially higher near the entrance than further downstream.

2.2 Fully Developed Region

In the fully developed region convective heat transfer leads to evaporation at the vapor/liquid interface. Chun and Seban [6] developed the following correlation for heat transfer to evaporating liquid films on smooth vertical tubes:

Laminar:

$$h_c = 0.821\left(\frac{\nu^2}{k^3 g}\right)^{\frac{1}{3}} \left(\frac{4\Gamma}{\mu}\right)^{-0.22} \tag{5a}$$

Turbulent:

$$h_c = 3.8 \times 10^{-3}\left(\frac{\nu^2}{k^3 g}\right)^{-\frac{1}{3}} \left(\frac{4\Gamma}{\mu}\right)^{0.4} \left(\frac{\nu}{\alpha}\right)^{0.65} \tag{5b}$$

Both correlations give the "local" heat transfer coefficient as a function of Reynolds number, $4\Gamma/\mu$. These correlations were shown in Ref. [6] to be consistent with inferences made from published condensation data. The laminar correlation, which is based on the condensation work of Zazuli, assumes that the effective film thickness is reduced by the action of capillary waves and ripples. The net effect is an increase in heat transfer when compared to Nusselt. The intersection of correlations (5a) and (5b) yields a pseudo-transition Reynolds number:

$$\left(\frac{4\Gamma}{\mu}\right)_{tr} = 5800\left(\frac{\nu}{\alpha}\right)^{-1.06} \tag{6}$$

This should not be regarded as an actual indication of the transition from laminar to turbulent but only as the point of transition from one correlation to the other. The actual transition to turbulence may be more accurately charaterized by the Weber number [6].

2.3 Nucleate Boiling

If the superheat is sufficiently high, boiling may occur in the film. It has been found that greater heat fluxes are attainable with boiling in thin films than with boiling in pools, e.g., [7-9]. Apparently the boiling mechanism in films is somewhat different from that in pools. Based on observations with high speed cinematography and simultaneous surface temperature measurements with special thermocouples, Messler [7] deduced that the excellent heat transfer in films was due to increased microlayer evaporation at the base of the growing bubbles. Others suggest that Marangoni effects may be important [8,9].

It was found [9] that the pool boiling curve is independent of liquid depth above a certain minimum depth. As the depth is reduced below this value the boiling curve shifts to the left (i.e., the heat transfer coefficient increases). In the case of water boiling at atmospheric pressure on horizontal surfaces, the minimum depth was found to be about 5 mm. The thickness of a falling film is generally more than an order of magnitude smaller than this value; consequently the boiling heat transfer coefficient will be greater than that for a pool configuration.

Experimental data for boiling of thin films is relatively scarce when compared to the abundance of data for boiling in pools. In view of this fact, it was decided to use pool boiling data to characterize boiling in thin films, with the knowledge that this modelling assumption is conservative. A widely accepted pool boiling correlation is that of Rohsenow [10,11] :

$$h_b = \frac{\mu\, h_{fg}}{C_{sf}^3 \sqrt{\frac{g_o}{g}\frac{\sigma}{\rho}}} \left[\frac{C_p}{h_{fg} P_r^s}\right]^3 \Delta T^2 \text{, where } s=1 \text{ for water}, \quad s=1.7 \text{ all other fluids} \tag{7}$$

and C_{sf} is a function of fluid-surface combination. This correlation will be employed in the present study. Experimental data, when available, will be used in preference to the Rohsenow correlation.

2.4 Overall Model for a Single Tube

The overall heat flux is assumed to be a superposition of convective heat transfer and boiling. This procedure is essentially similar to that of Bergles and Rohsenow [12] for determining forced convective boiling heat transfer coefficients. The average heat transfer coefficient over the circumferential length L is then:

$$\bar{h} = \underbrace{h_b}_{\substack{\text{boiling over}\\ \text{entire length}}} + \underbrace{h_d \frac{L_d}{L}}_{\substack{\text{convection in}\\ \text{developing region}}} + \underbrace{h_c \left[1 - \frac{L_d}{L}\right]}_{\substack{\text{convection in}\\ \text{fully developed}\\ \text{region}}} \tag{8}$$

where,

$$h_b = \frac{\mu\, h_{fg}}{C_{sf}^3 \sqrt{\frac{g_o}{g}\frac{\sigma}{\rho}}} \left[\frac{C_p}{h_{fg} P_r^s}\right]^3 \Delta T^2 \tag{8a}$$

$$h_d = \frac{3}{8} C_p \frac{\Gamma}{L_d} \tag{8b}$$

$$L_d = \frac{\Gamma^{4/3}}{4\pi\rho\alpha} \sqrt[3]{\frac{3\mu}{g\rho^2}} \tag{8c}$$

Laminar:

$$h_c = 0.821 \left(\frac{\nu^2}{k^3 g}\right)^{-\frac{1}{3}} \left(\frac{4\Gamma}{\mu}\right)^{-0.22} \tag{8d}$$

Turbulent:

$$h_c = 3.8 \times 10^{-3} \left(\frac{\nu^2}{k^3 g}\right)^{-\frac{1}{3}} \left(\frac{4\Gamma}{\mu}\right)^{0.4} \left(\frac{\nu}{\alpha}\right)^{0.65} \tag{8e}$$

Since $\bar{h}$ is defined as the average heat transfer coefficient over the entire length, it should be evident that the quantities (L_d/L) and $(1 - L_d/L)$ in equation (8) merely weight the convection heat transfer components according to length over which each is effective. Equations (8d) and (8e) are evaluated assuming a constant flowrate, a procedure which does not take into account the thinning of the film. Comparisons with a more exact differential formulation indicated that the constant flowrate assumption is good as long as the amount of fluid evaporated is small compared to the feed flowrate.* In the worst case (i.e., at the flowrate leading to dryout at the bottom of the tube) the simple model underpredicts the heat transfer coefficient by about 25%. At higher feed flowrates the simple model differs from the more exact formulation by only a few percent. All predictions presented in this paper are determined from the exact model, although reference is made to equation (8). Except when boiling is present in the film, the predicted heat transfer coefficient is not extremely sensitive to superheat, ΔT. The value of ΔT is important only inasmuch as it determines the flowrate at which dryout occurs. For cases with no boiling in the film, calculations are made with $\Delta T = 6.0°C$ and $2.8°C$ for water and ammonia, respectively. When boiling is present, the superheat employed for the calculations will be specified in each case.

2.5 Vertical Bank of Horizontal Tubes

In the case of a vertical bank of horizontal tubes, the unevaporated fluid from any given tube is assumed to fall on the next lower tube, see Figure 1. The behavior of a tube bank is complicated by the influence of between-tube evaporation and turbulence generated as liquid falls from one tube to the next. Also vapor crossflow can be important. A conservative estimate of the heat transfer behavior of a tube bank can be obtained by neglecting between-tube evaporation and turbulence, and extending the analysis for a single tube. If the bank is fed by liquid at T_s, the temperature profile generally becomes fully developed somewhere on the uppermost tube. Thus the behavior of the top tube is similar to that of a single isolated tube and the model of the previous section is directly applicable. The liquid reaching the second tube has been superheated by the first tube and therefore no developing length is required. Accordingly the heat transfer coefficient on the second tube is simply given by the Chun-Seban correlation (i.e., h_c) if no boiling occurs or $h_b + h_c$ if boiling is present. The heat transfer coefficients of all lower tubes are determined in a similar manner, with h_c for any given tube calculated using the local flowrate Γ of liquid reaching that tube. The average heat transfer coefficient for the entire tube bank is then the arithmetic average of the heat transfer coefficients of all the individual tubes. This procedure for calculating the average heat transfer coefficient for a bank of n tubes is equivalent to employing equation (8) with an effective length of $L = n\pi d/2$.

*See Appendix A for a description of the differential formulation.

The foregoing procedure neglects the influence of between-tube evaporation. The liquid film has an average superheat of $\sim \frac{3}{8} \Delta T$ and in falling from one tube to the next a portion of that superheat is removed by evaporation. A simple model of between-tube evaporation was developed by assuming that the liquid falls as a uniform sheet with a thickness equal to twice the film thickness on the tube. A Kantrovich method was employed to solve the transient heat conduction problem with respect to an observer travelling with the falling liquid. The time of flight between tubes was calculated assuming that the liquid falls as a free body. For the small tube spacings presently being considered for OTEC (i.e., less than 2.54 cm) the model indicated an increase in heat transfer of no more than about 15%. If the tube spacing is large, between-tube evaporation can be more important. The limiting case is where all the superheat is removed by between-tube evaporation. If this occurs the next lower tube will behave as a single tube fed by fluid at T_s. Thus single tube predictions can be regarded as an upper limit for heat transfer to any given tube in the bank.

For condensation on vertical banks of horizontal tubes, Chen [13] used a between-tube condensation model to explain why the Nusselt equation underpredicts heat transfer coefficients on the lower tubes. A more popular explanation is that the good heat transfer is a result of turbulence produced by dripping and splashing of the condensate. It is logical to assume that a similar mechanism occurs in evaporators. Liu [3] found that the heat transfer coefficient increases with tube spacing, but is not strongly dependent on flowrate. According to Liu the initial liquid velocity at the top of a tube is the critical factor in determining heat transfer behavior. Since the liquid velocity depends on the falling distance, and not on the flowrate, the observed behavior appeared to be reasonable.

Neglecting the influence of between-tube evaporation and turbulence generated by the falling liquid will lead to a conservative prediction. With the relatively small tube spacings being considered for OTEC, the influence of between-tube evaporation and turbulence may not be extremely significant; but without supporting experimental evidence, the potential importance of these effects cannot be discounted. Perhaps the safest characterization of heat transfer to any given tube is to assume that the actual value is bounded above by the single tube prediction and below by the fully developed correlation of Chun-Seban.

Before closing this section a few remarks should be made regarding vapor velocity. The influence of a downward flow of vapor was studied analytically by Liu [3]. It was found that vapor shear effects become important only at high vapor velocities. For example, with a 2.54 cm diameter tube and a water feed flowrate of $\Gamma = 0.15$ kg/s-m at $T_s = 100°C$, the increase in heat transfer coefficient is less than 10% for vapor flowrates up to 9.1 m/s. Liu considered vapor downflow (and upflow) but not vapor crossflow. A high crossflow velocity can cause deflection of liquid away from the tubes. Also liquid may be stripped from the tubes and entrained into the vapor flow. These effects, among others, can cause redistribution of liquid and incomplete wetting of the tubes. A detailed study of this problem is presently being conducted by the authors.

3.0 Results

The single tube experiments of Fletcher et al. [1,2] and Liu [3] provide data that can be used to verify the present analysis. Using the apparatus shown in Figure 4a, Fletcher measured heat transfer coefficients for thin films of distilled water [1] and sea water [2] on horizontal tubes. Feedwater at T_s was delivered via a perforated plate onto an electrically heated horizontal tube. Average heat transfer coefficients were determined from the heat input, feedwater saturation temperature, and the average tube wall temperature as determined from thermocouples located circumferentially and axially along the tube. Except for having a more elaborate feed distribution system, the experimental apparatus of Liu, Figure 4b, is similar to that of Fletcher. Liu's apparatus has the added advantage of being able to simulate different tube spacings.

Figure 5 shows a comparison of predictions with experimental data for the case of no boiling in the film. For this comparison only the low heat flux, low ΔT data of Fletcher [1] is plotted, because at higher heat fluxes boiling was observed. The data of Liu is also for runs where no boiling was observed. Liu obtained data over a range of tube spacings but only data for spacing less than a 2.54 cm is plotted. Tube spacings greater than this are beyond the present range of interest for OTEC.

As observed in Figure 5, the present analysis is in good agreement with the data. The trends indicated by the model are rather interesting. At low flowrates, $\bar{h}$ is large because the film is relatively thin. (The lowest flowrate plotted in the figure is that which leads to dryout at $z = L$.) As the flowrate increases, the film thickens and consequently $\bar{h}$ decreases. At still higher flowrates heat transfer in the developing regions becomes increasingly important, and $\bar{h}$ gradually rises. The variance between the Chun-Seban correlation and the present model reflects the influence of the thermal developing region. Note the large divergence at high flowrates where the developing length is most important. For reference the Nusselt prediction is also plotted.

A plot of heat transfer coefficient versus position at a typical flowrate is given in Figure 6. For this case the average heat transfer coefficient in the developing region is about 2.7 times the heat transfer coefficient in the fully developed region. This general behavior is analogous to convective heat transfer in pipes where the heat transfer coefficient is high near the entrance and approaches a fully developed value further downstream. In Figure 6, note that the developing length covers about 35% of the total circumferential length L.

The experimental data plotted in Figures 7 and 8 covers a wide range of superheats. The vertical bands around the data reflect a ΔT dependence which is indicative of boiling. In Figure 8 some of the data points have large vertical bands while others have relatively small bands. This kind of variability is often found in boiling data and is attributable to ageing, wettability, contamination, nucleation site stability, and hysteresis. As seen in Figures 7 and 8, predictions using the present model bound the

data very well. The lower bound is calculated by assuming no boiling in the film. The upper bound is calculated by introducing nucleate boiling and evaluating the boiling heat transfer coefficient h_b at the highest superheat; i.e., $\Delta T = 6.78°C$ in Figure 7 and $\Delta T = 6.0°C$ in Figure 8. In evaluating the boiling heat transfer coefficient, equation (8a) was employed with values of C_{sf} consistent with the recommendations of Rohsenow and others [9-11]. Values of $C_{sf} = 0.0154$ and 0.0122 were used in calculating h_b for the 2.54 cm and 5.08 cm diameter tubes, respectively.

To our knowledge, the present model is the first to successfully predict Fletcher's data. Fletcher found that neither the pool boiling nor convective mechanism alone could account for the behavior of the data. He made no attempt to combine the boiling and convective components. In the present model, the data was successfully predicted by a superposition of boiling and convection, and including the influence of the thermal developing region.

In view of the fact that the present analysis adequately predicts water data, the model will now be extended to ammonia, which is the most commonly selected working fluid for the OTEC power cycle. Figure 9 shows the predicted behavior of ammonia for a situation where no boiling occurs in the film. The general trend is similar to that of water, but the magnitude of $\bar{h}$ is less. A plot of heat transfer coefficient versus position at a given flowrate is given in Figure 10. For this case the average heat transfer coefficient in the thermal developing region is 2.8 times the heat transfer coefficient in the fully developed region. The developing length covers about 38% of the length L. (Recall for water that $h_d/h_c = 2.7$ and $L_d/L = 0.35$).

It was previously noted that equation (8) with $L = n\pi d/2$ provides a conservative estimate of the heat transfer coefficient for a bank of n tubes. Following this approach, Figure 11 gives predictions for tube banks ranging from n = 10 to 100. The prediction for a single tube is shown for reference. Over the range plotted, a negligible influence of bank size is observed as all the predictions approach the Chun-Seban correlation. The only notable effect of bank size is the flowrate at which dryout occurs.

Referring back to Figure 9, some interesting observations can be made regarding the behavior of a tube bank. The single tube prediction is representative of the first tube in the bank. The Chun-Seban correlation is representative of the behavior of lower tubes if between-tube evaporation and turbulence resulting from the falling liquid are negligibly small. If these effects are significant then the heat transfer coefficient for the bank may approach that of a single tube. In view of this uncertainty, caution should be exercised when using results of single tube experiments to characterize the behavior of an entire bank. To accurately assess the influence of between-tube evaporation and turbulence we recommend that experiments be performed with a bank of at least three tubes. These remarks pertain essentially to plain tubes which have relatively low heat transfer coefficients. For enhanced surfaces with high heat tranfer coefficients, the potential improvement in $\bar{h}$ resulting from between-tube evaporation and turbulence is relatively small, see Figure 12.

Predictions given thus far for ammonia have been for the case where no boiling occurs in the film. It is difficult to initiate boiling with ammonia because it wets surfaces very well and floods out nucleation sites. A number of enhancement techniques have been used to create stable re-entrant cavities. Sabin and Popendiek [14] have experimented with double-screen tube coverings and Czikk et al. [15] with porous metal coatings (i.e.,Linde High Flux surface). With the Linde High Flux surface, boiling of ammonia was observed even at the lowest measureable superheats. The experimentally measured boiling heat transfer coefficient was nearly constant at about h_b = 34.1 kW/m^2-K. Figure 12 shows predictions for an enhanced tube with h_b = 34.1 kW/m^2-K. Compared to plain tubes, the increase in heat transfer coefficient is nearly ten-fold. Most of the increase is, of course, attributable to the large boiling component. For simplicity let each curve in Figure 12 be characterized by its minimum value. With this characterization, the upper and lower limits of $\bar{h}$ for a bank of plain tubes are 5.6 kW/m^2-K and 3.1 kW/m^2-K, respectively.

Recall that the upper limit will be approached when between-tube evaporation and turbulence are important, and the lower limit when these effects are negligible. For a bank of enhanced tubes the upper and lower limits of $\bar{h}$ are 39.5 kW/m^2-K and 37.2 kW/m^2-K, respectively. This small spread in $\bar{h}$ is indicative of the fact that the boiling dominates over convection.

Before closing the discussion on enhancement, it should be pointed out that boiling enhancement is not the only means for obtaining relatively high heat transfer coefficients on horizontal tubes. Schultz et al. [4] obtained a coefficient of about 18.7 kW/m^2-K by threading the tubes. Although the mechanism responsible for this improvement was not given, it is probably attributable to intermittent wetting of crests by waves and subsequent evaporation of the thin liquid film which is left behind.

Figure 13 shows a plot of the overall U for an OTEC evaporator with a water side heat transfer coefficient of 5.7 kW/m^2-K (no enhancement), a fouling conductance of 22.7 kW/m^2-K, and a wall conductance of 56.8 kW/m^2-K. The ammonia side coefficient as a function of flowrate is taken from Figure 12. Characterizing each curve by its minimum value, the upper and lower limits of U are 2.33 kW/m^2-K and 1.82 kW/m^2-K respectively for plain tubes. With the enhanced tubes the upper and lower limits are essentially coincident at a value of about 3.8 kW/m^2-K.

4.0 Conclusions

A model of combined boiling and evaporation of liquid films on horizontal tubes was developed. The results of this work are applicable to the design of horizontal tube falling film evaporators for OTEC. In modelling the behavior of single tubes, special account must be taken of the initial thermal developing region of the film. Predictions agreed favorably with the published experimental data of Fletcher et al. [1,2] for combined boiling and evaporation of thin water films on single horizontal tubes. To our knowledge this is the first model to successfully predict Fletcher's data.

The predicted upper and lower limits of heat transfer for ammonia on a vertical bank of plain tubes are 5.4 kW/m^2-K and 3.1 kW/m^2-K, respectively. The upper limit will be approached when the influence of between-tube evaporation and turbulence created by liquid falling from one tube to the next are important. Tests with single tubes are inadequate to assess the influence of between-tube evaporation and turbulence. We recommend that future experiments be performed with a bank of at least three tubes. The experimental work should also consider the influence of vapor crossflow.

For an OTEC evaporator with plain tubes, the upper and lower limits of the overall U are 2.33 kW/m^2-K and 1.82 kW/m^2-K, respectively. With ammonia-side boiling enhancement, the overall U can be increased to about 3.8 kW/m^2-K.

References

1. Fletcher, L. S., Sernas, V., Galowin, L. S., "Evaporation from Thin Water Films on Horizontal Tubes," ASME Paper No. 73-HT-42, ASME-AIChE Heat Transfer Conference, Atlanta, Georgia, 1973.

2. Fletcher, L. S., Sernas, V., Parken, W. H., "Evaporation Heat Transfer Coefficients for Thin Sea Water Films on Horizontal Tubes," Ind. Eng. Chem., Process Des. Dev., Vol. 14, No. 4, 1975.

3. Liu, P., "The Evaporation Falling Film on Horizontal Tubes," PhD dissertation, Univ. of Wisconsin, 1975.

4. Schultz, V. N., Edwards, D. K., and Catton, I. "Experimental Determination of Evaporative Heat Transfer Coefficients on Horizontal Threaded Tubes," AIChE Symposium Series, No. 164, Vol. 73, 1977.

5. Moalem, D. and Sideman, S., "Theoretical Analysis of a Horizontal Condenser-Evaporator Tube," Int. J. Heat Mass Transfer, Vol. 19, 1976.

6. Chun, K. R. and Seban, R. A., "Heat Transfer to Evaporating Liquid Films," Journal of Heat Transfer, Trans. ASME, Series C, Vol. 93, 1971.

7. Messler, R., "A Mechanism Supported by Extensive Experimental Evidence to Explain High Heat Fluxes Observed During Nucleate Boiling," AIChE Journal, Vol. 22, No. 2, 1976.

8. Nishikawa, K., Kusada, H., Yamasaki, K., and Tanaka, K., "Nucleate Boiling at Low Liquid Levels," Bull. JSME, 10, 1976.

9. Marto, P. J., MacKensie, D. K., and Rivers, A. D., "Nucleate Boiling in Thin Liquid Films," AIChE Symposium Series, No. 164, Vol. 73, 1977.

10. Rohsenow, W. M., "A Method of Correlating Heat Transfer Data for Surface Boiling of Liquids," Trans. ASME, Vol. 74, 1952.

11. Rohsenow, W. M.,"Discussion on the Rohsenow Pool Boiling Correlation," Journal of Heat Transfer, Trans. ASME, Series C, Vol. 94, 1971.

12. Bergles, A. E. and Rohsenow, W. M., "The Determination of Forced-Convective-Surface-Boiling Heat Transfer Journal of Heat Transfer, Trans. ASME, Series C, Vol. 86, 1964.

13. Chen, M. M., "An Analytical Study of Laminar Film Condensation," Journal of Heat Transfer, Trans. ASME, Series C, Vol. 83, 1961.

14. Sabin, C. M. and Poppendiek, H. F., "Heat Transfer Enhancement for

Evaporators," Proceedings, Fourth Annual Conference on OTEC, New Orleans, La., 1977.

15. Czikk, A. M., Fricke, H. D., and Ganic, E. N., "Enhanced Performance Heat Exchangers," Proceedings, Fourth Annual Conference on OTEC, New Orleans, La., 1977.

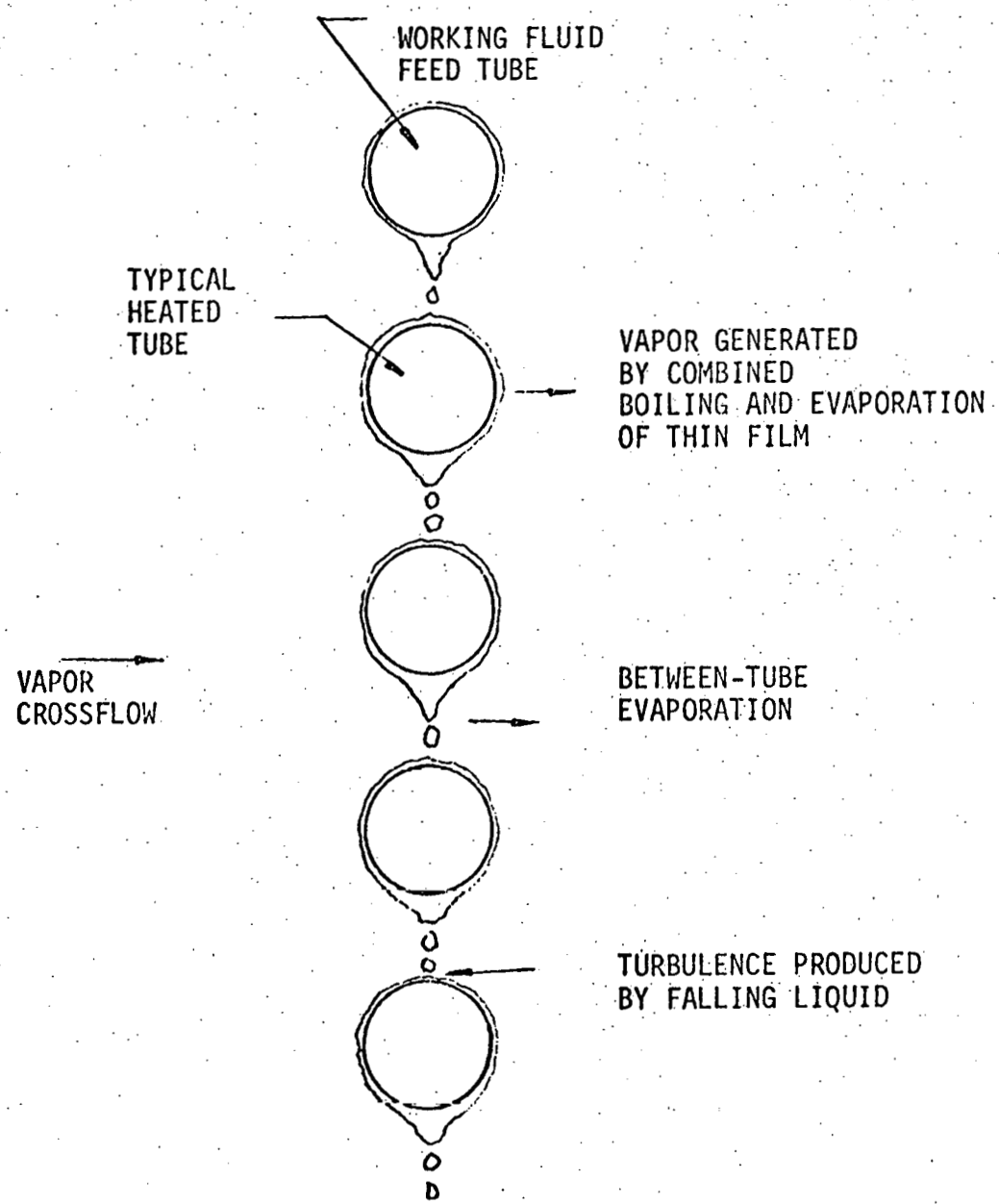

FIGURE 1. UPPER PORTION OF VERTICAL BANK OF HORIZONTAL TUBES

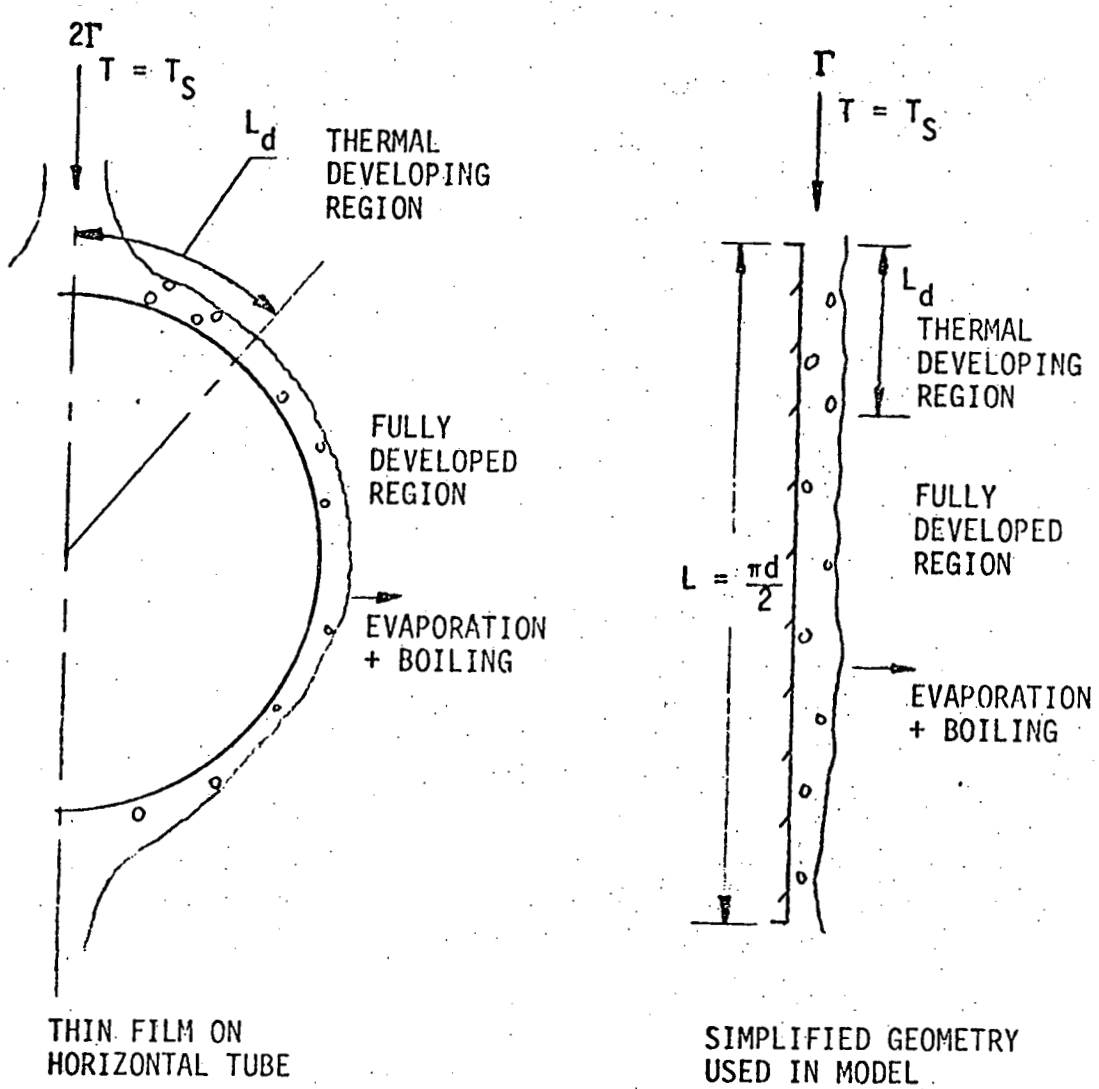

FIGURE 2. SKETCH OF ACTUAL CONFIGURATION AND SIMPLIFIED GEOMETRY USED IN MODEL

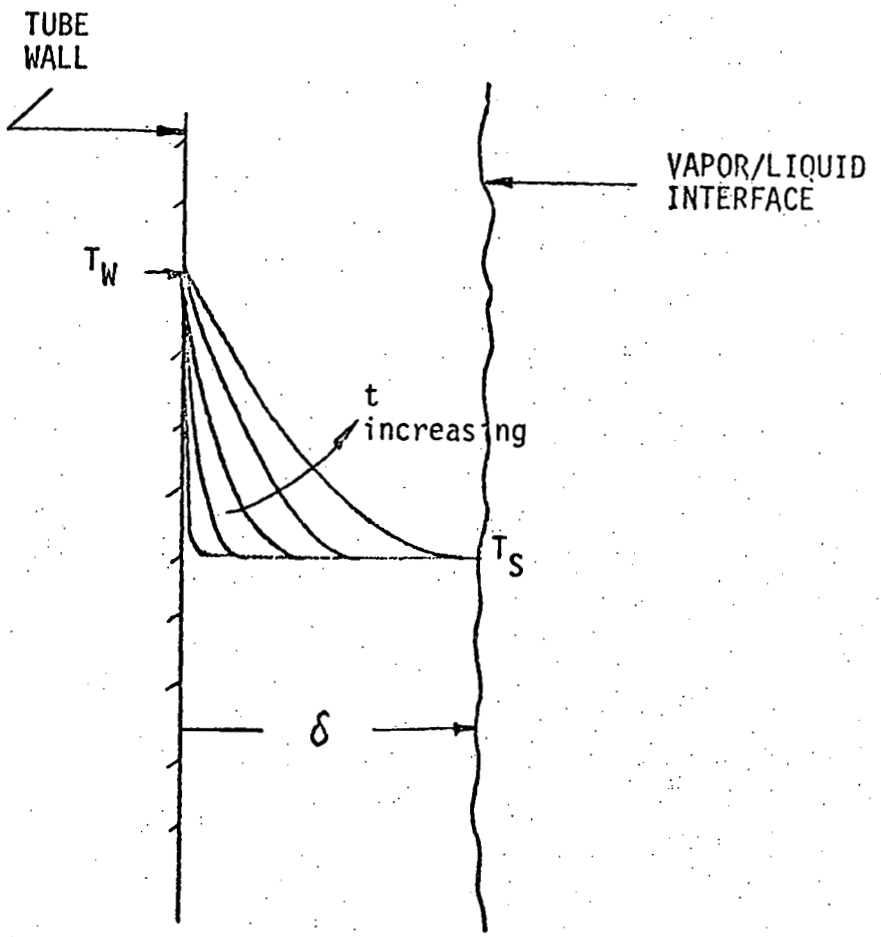

FIGURE 3. DEVELOPMENT OF TEMPERATURE PROFILE TO AN OBSERVER MOVING WITH THE AVERAGE FILM VELOCITY

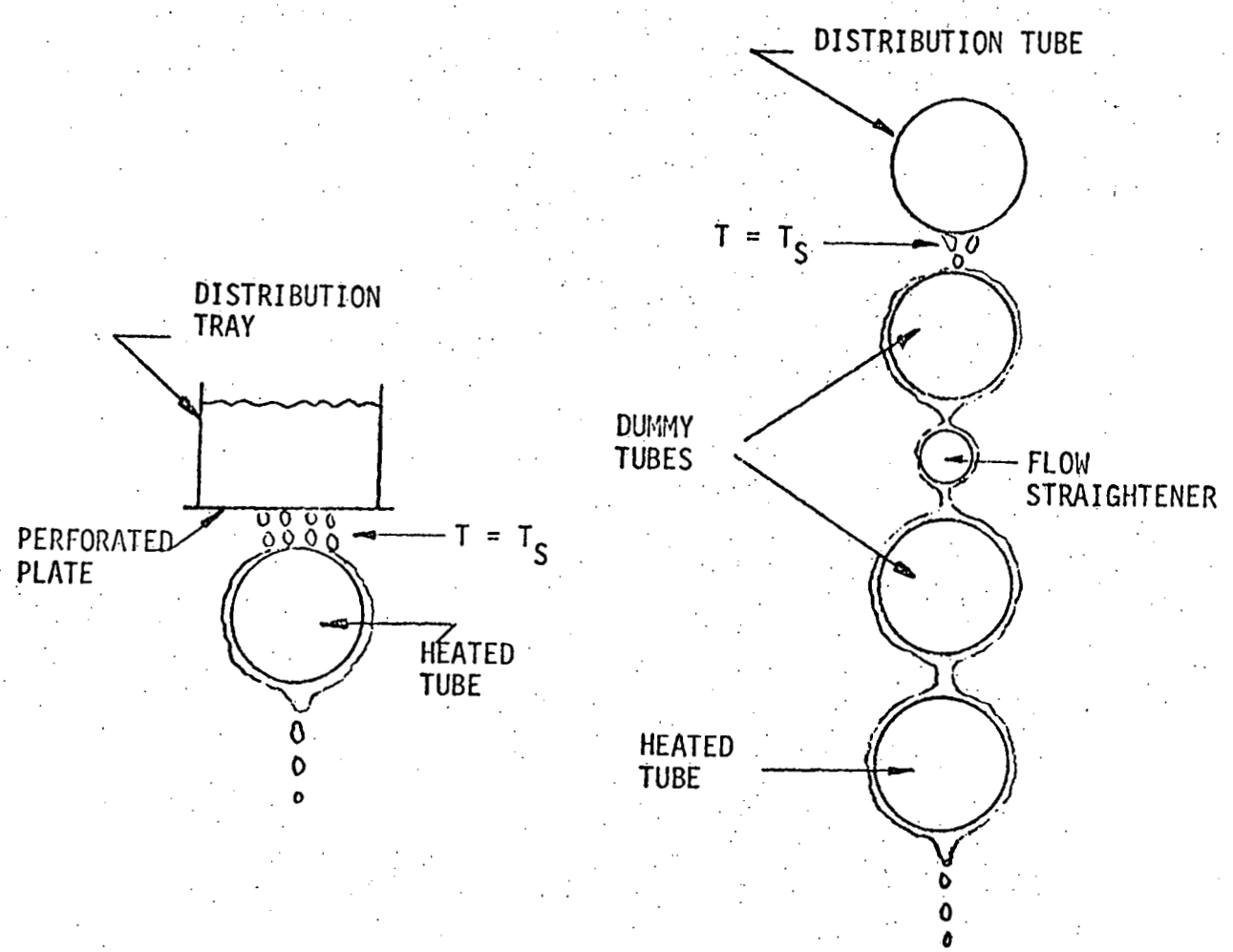

(a) DISTRIBUTION SYSTEM OF FLETCHER [1]

(b) DISTRIBUTION SYSTEM OF LIU [3]

FIGURE 4. EXPERIMENTAL APPARATUS OF FLETCHER [1] AND LIU [3]

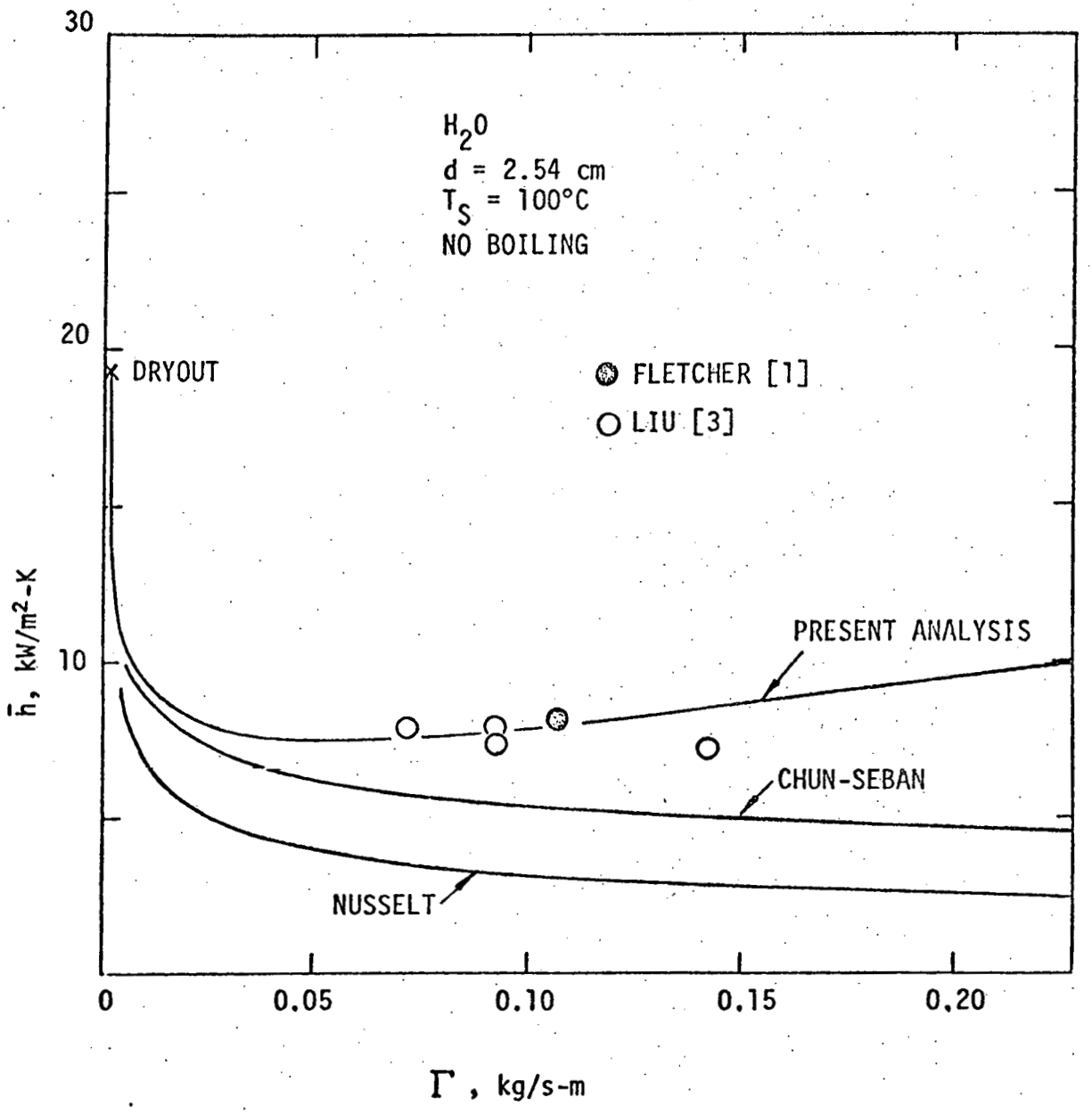

FIGURE 5. COMPARISON OF PREDICTIONS WITH EXPERIMENTAL DATA OF FLETCHER [1] AND LIU [3]

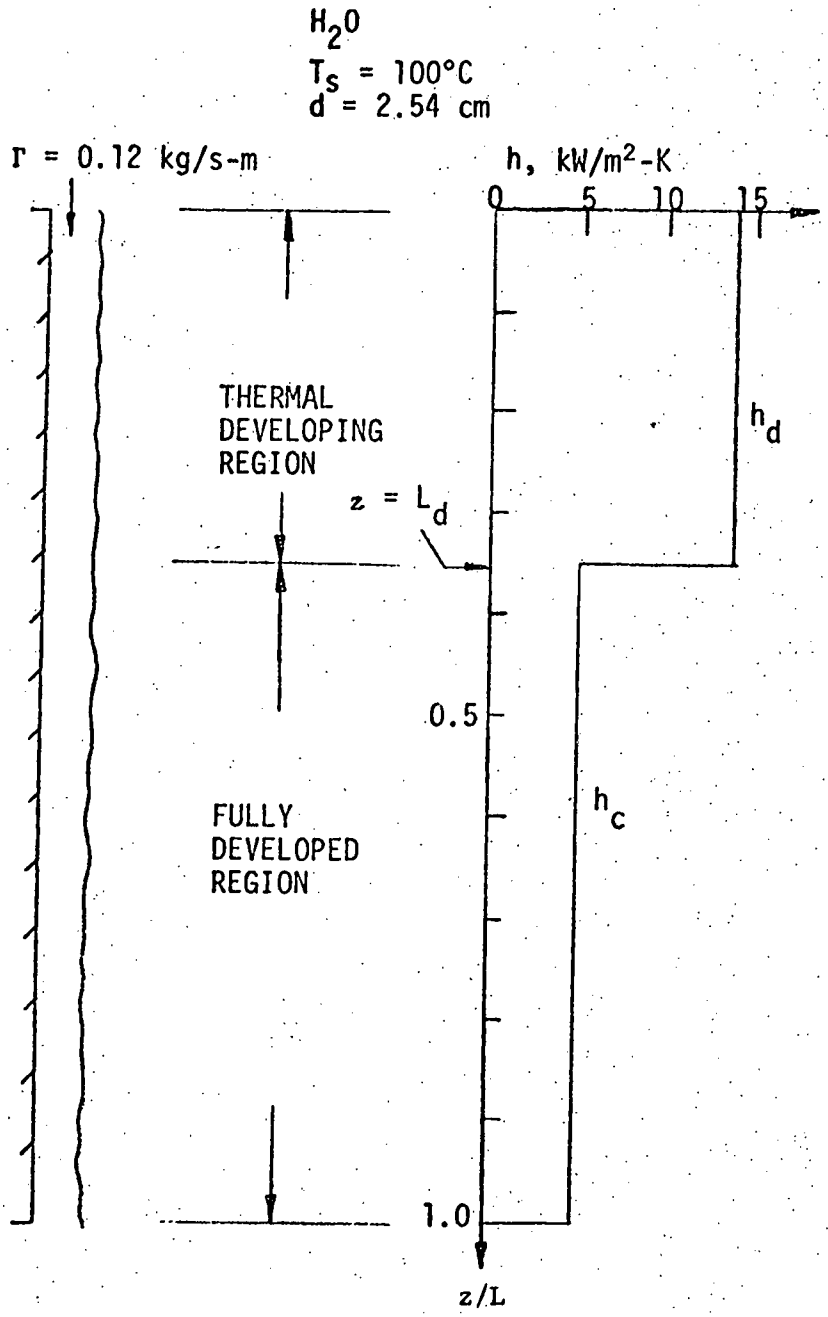

FIGURE 6. VARIATION OF HEAT TRANSFER COEFFICIENT WITH POSITION

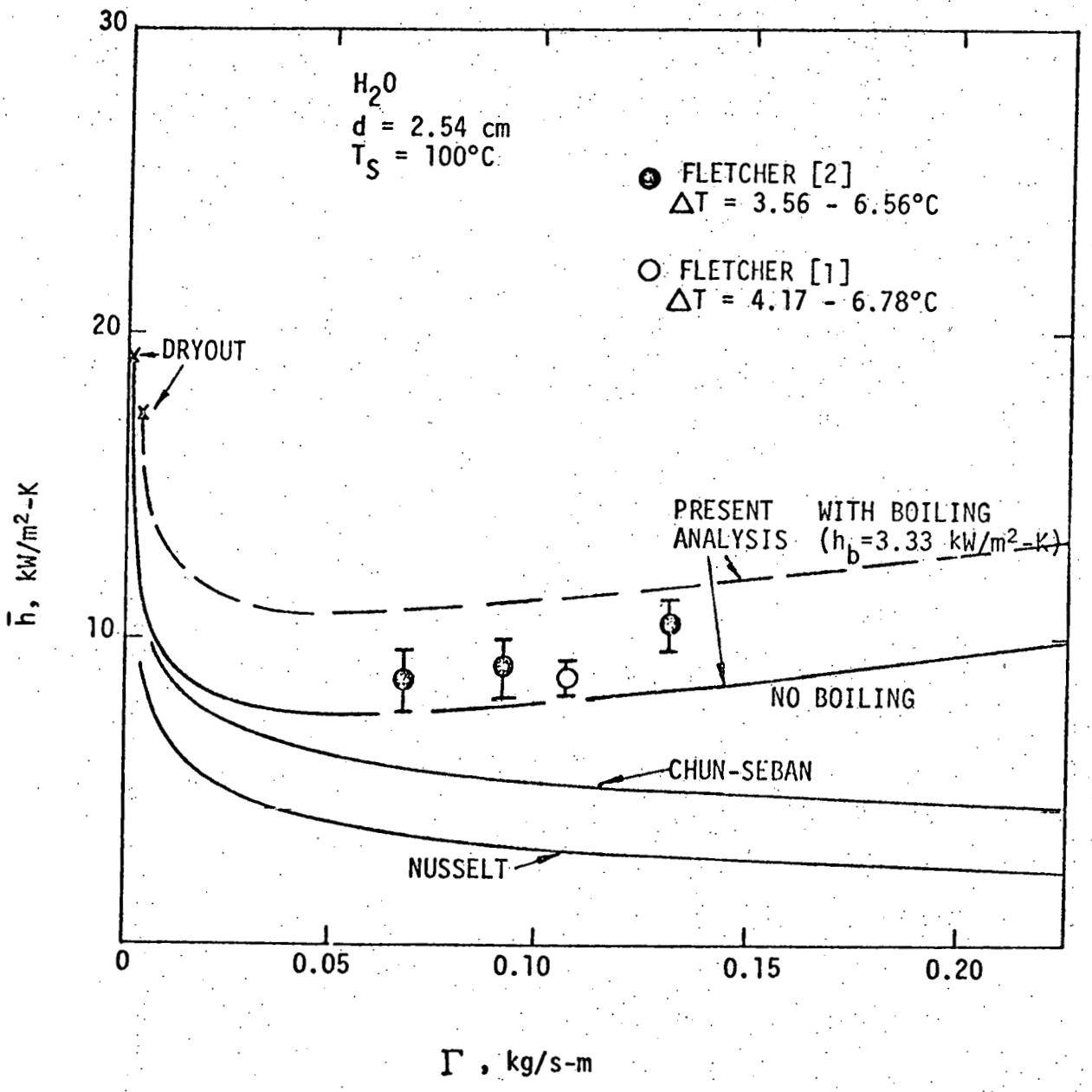

FIGURE 7. COMPARISON OF PREDICTIONS WITH EXPERIMENTAL DATA OF FLETCHER [1,2]

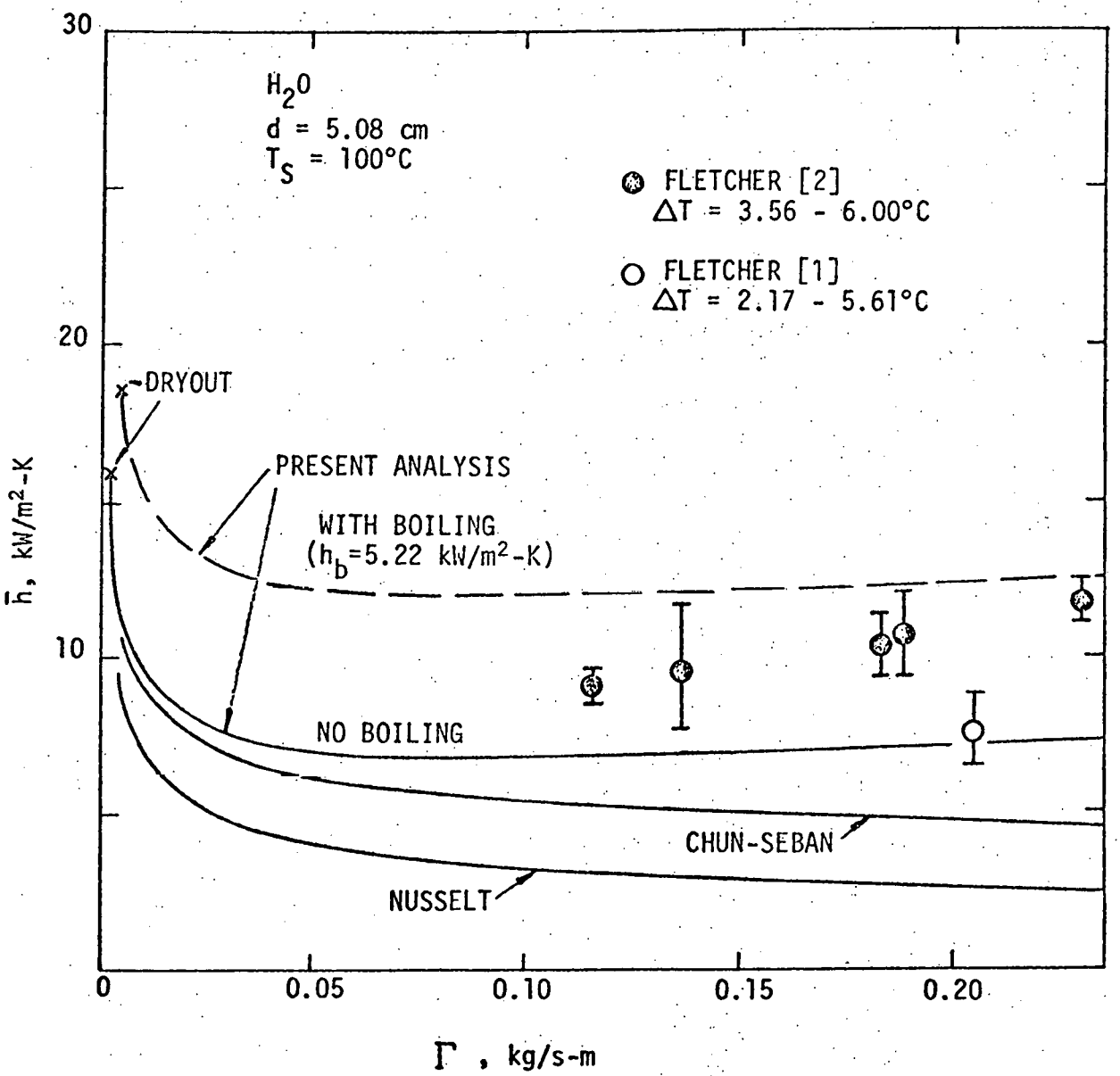

FIGURE 8. COMPARISON OF PREDICTIONS WITH EXPERIMENTAL DATA OF FLETCHER [1,2]

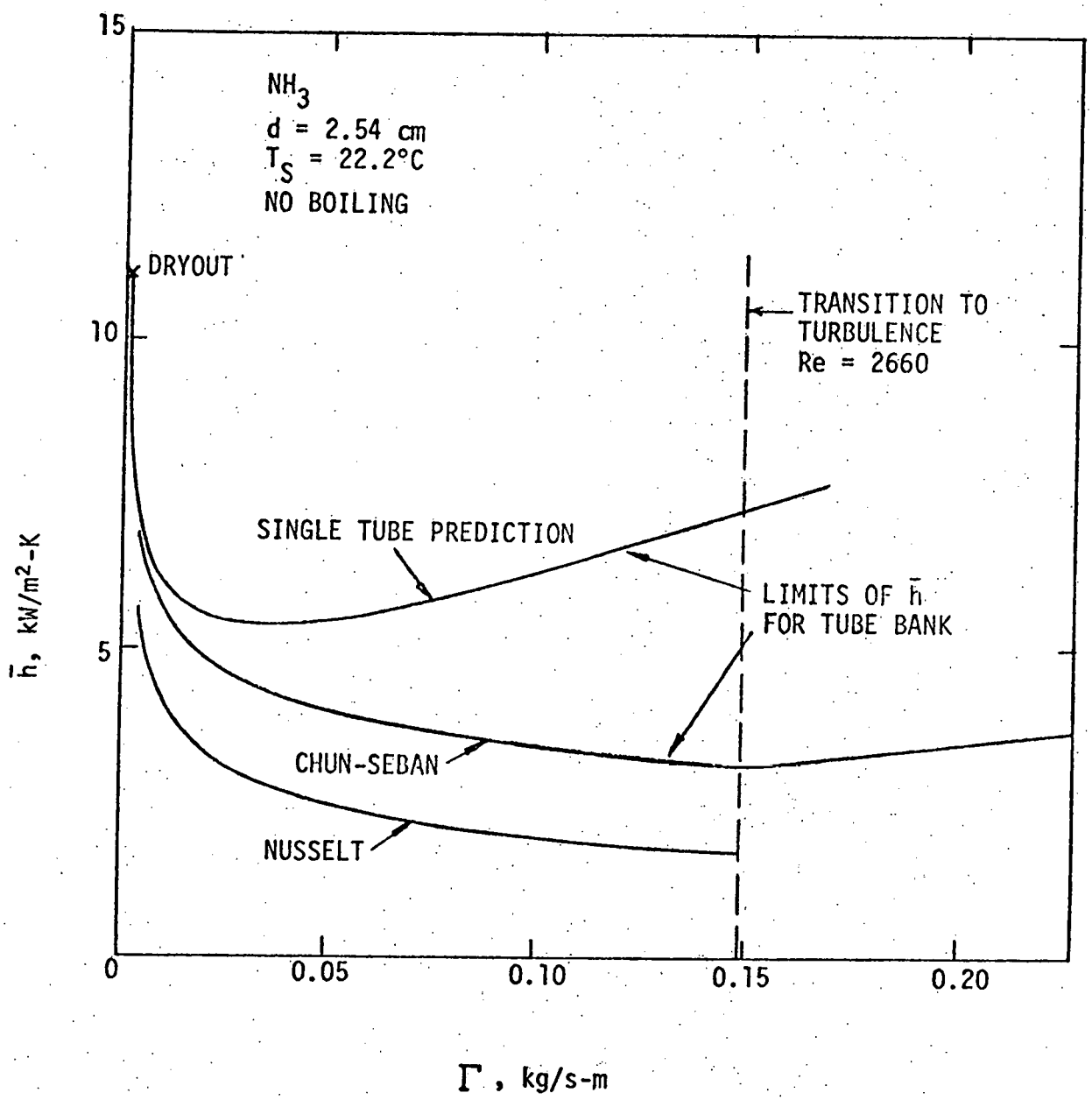

FIGURE 9. PREDICTED BEHAVIOR OF AMMONIA ON PLAIN TUBES WITH NO BOILING

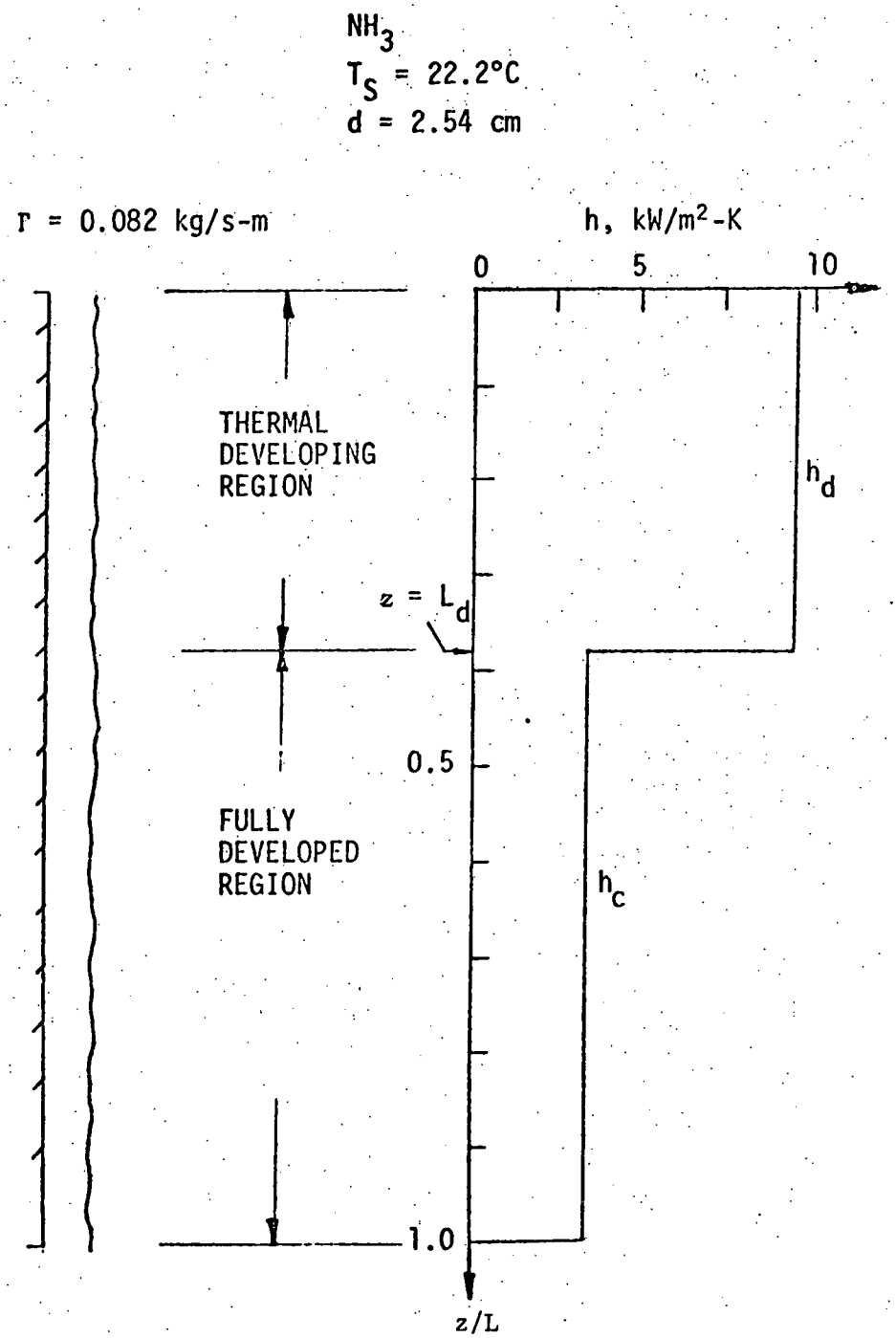

FIGURE 10. VARIATION OF HEAT TRANSFER COEFFICIENT WITH POSITION

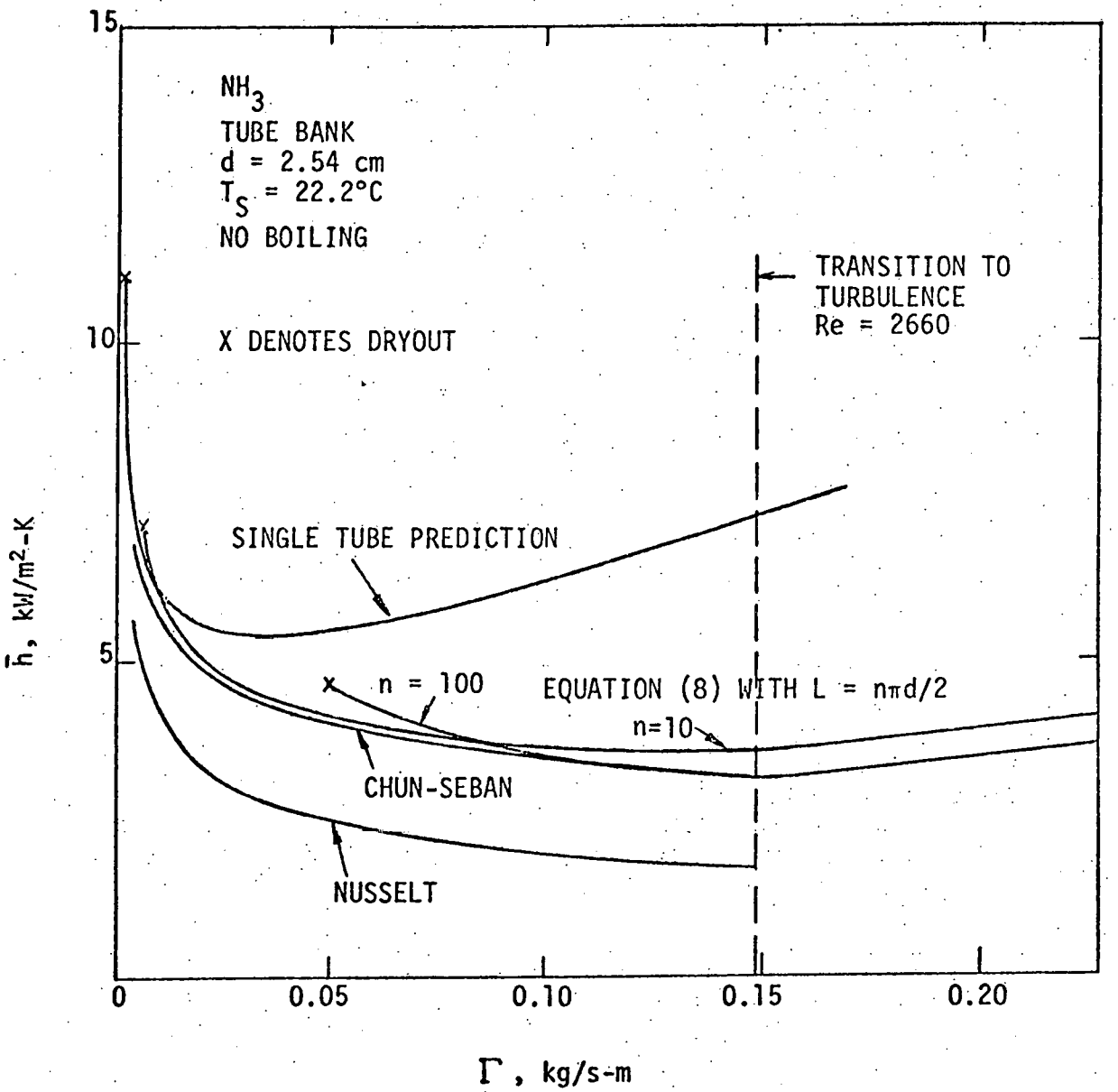

FIGURE 11. PREDICTED BEHAVIOR OF AMMONIA ON VERTICAL BANKS OF PLAIN TUBES

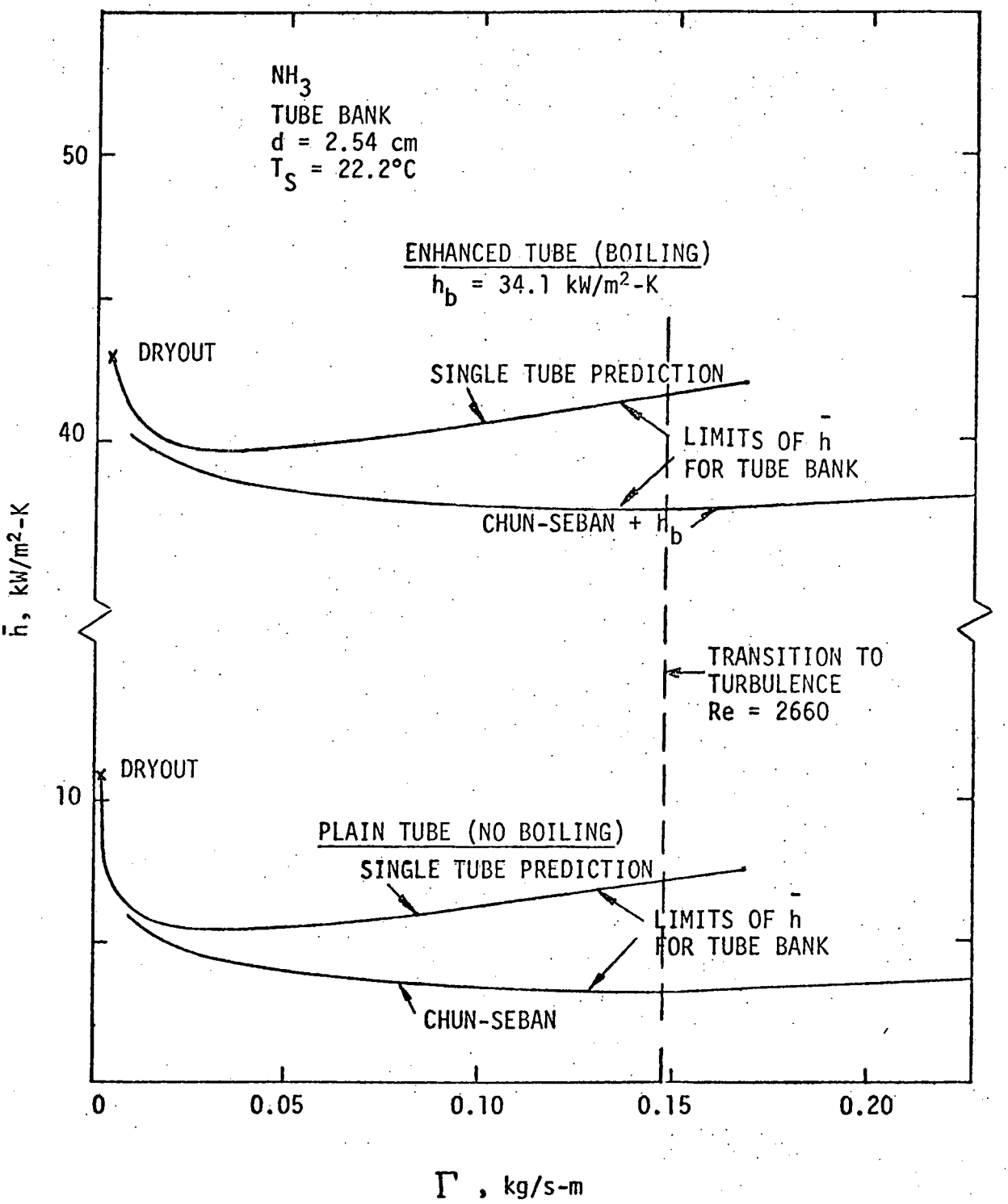

FIGURE 12. PREDICTED BEHAVIOR OF AMMONIA ON VERTICAL BANKS OF ENHANCED AND PLAIN TUBES

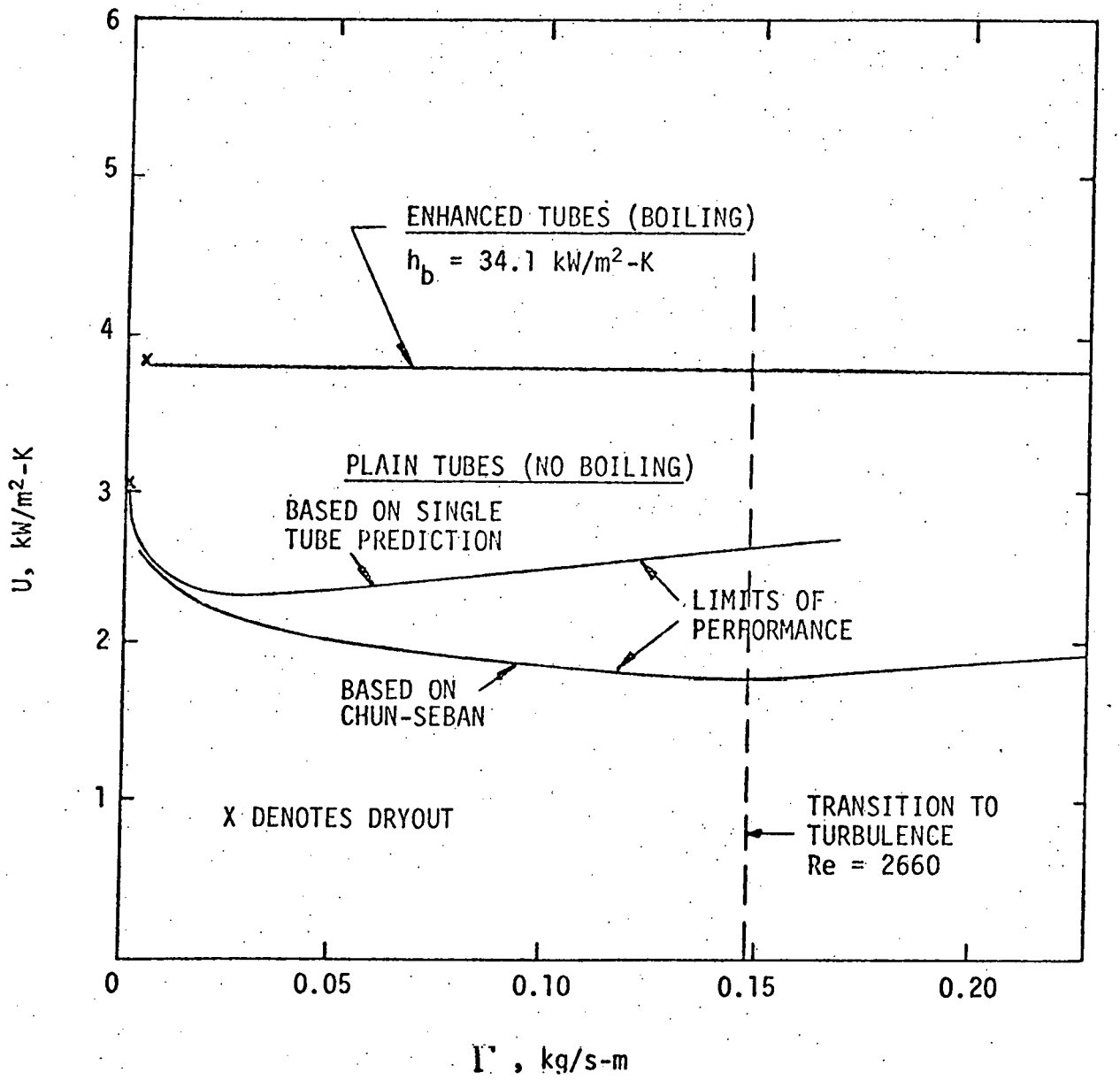

FIGURE 13. PREDICTED OVERALL U FOR AN OTEC EVAPORATOR WITHOUT WATER SIDE ENHANCEMENT

Appendix A

In Section 2.4 it was indicated that equation (8) constitutes a simple model when the decrease in Γ with z is neglected. The influence of flowrate will be reflected in the value of h_c, which in the more exact differential formulation is no longer given by equations (8d) and (8e). Values of h_b and h_d are essentially independent of flowrate variations and thus are still given by equations (8a) and (8b), respectively. The purpose of this Appendix is to present the differential formulation for the heat transfer coefficient in the fully developed region, i.e., h_c. Both laminar and turbulent cases will be considered. Finally predictions with the simple model will be compared with predictions using the differential model.

A.1 Laminar Case

In the region $L>z>L_d$, the temperature profile is fully developed and vapor is generated by combined boiling and evaporation. For a single tube of diameter d, the length is defined as $L = \pi d/2$. (For a bank of n tubes, a lower limit of performance can be obtained by defining the effective length as $L = n\pi d/2$, see discussion in Section 2.5.) An energy balance on a differential element yields:

$$\frac{q_b}{A} + \frac{q_c}{A} = -\frac{d\Gamma}{dz} h'_{fg} \tag{A1}$$

where

$$h'_{fg} = h_{fg} - \frac{3}{8} C_p \Delta T \tag{A2}$$

and q_b/A is the heat transfer due to boiling, given by equation (8a). Equation (A1) will be evaluated using two different expressions for q_c/A, first the conventional Nusselt expression and secondly the Chun-Seban correlation.

A.1.1 Formulation Using the Nusselt Expression

The Nusselt expression for q_c/A is given as follows:

$$\frac{q_c}{A} = k \frac{\Delta T}{\delta} = k\Delta T \left(\frac{3}{4} \frac{\nu^2}{g}\right)^{-\frac{1}{3}} \left(\frac{4\Gamma}{\mu}\right)^{-\frac{1}{3}} \tag{A3}$$

Substituting equation (A3) into equation (A1) gives a first order differential equation which can be integrated subject to the boundary condition $\Gamma = \Gamma_o$ at $z = L_d$ to yield:

$$\frac{4}{3}\left[\left(1 + B_o Re_o^{\frac{1}{3}}\right)^3 - \left(1 + B_o Re^{\frac{1}{3}}\right)^3\right] - 6\left[\left(1 + B_o Re_o^{\frac{1}{3}}\right)^2 - \left(1 + B_o Re^{\frac{1}{3}}\right)^2\right]$$

$$+ 12\left[\left(1 + B_o Re_o^{\frac{1}{3}}\right) - \left(1 + B_o Re^{\frac{1}{3}}\right)\right] - 4\left[\ln\left(1 + B_o Re_o^{\frac{1}{3}}\right) - \ln\left(1 + B_o Re^{\frac{1}{3}}\right)\right]$$

$$= B_o^4 \frac{(z-L_d)}{D_o} \tag{A4}$$

where

$$Re = \frac{4\Gamma}{\mu}; \quad Re_o = \frac{4\Gamma_o}{\mu} \tag{A5}$$

$$B_o = \frac{(q_b/A)}{k\,\Delta T}\left[\frac{3\nu^2}{4g}\right]^{\frac{1}{3}} \tag{A6}$$

$$D_o = \frac{h'_{fg}\,\rho g}{4\nu k\,\Delta T}\left[\frac{3\nu^2}{4g}\right]^{\frac{4}{3}} \tag{A7}$$

The average value of q_c/A over $L_d \leq z \leq L$ is

$$\frac{\bar{q}_c}{A} = \frac{1}{(L-L_d)}\int_{L_d}^{L} \frac{q_c}{A}\, dz \tag{A8}$$

Using the method of integration by parts, equation (A8) can be integrated to obtain the average heat transfer coefficient, h_c:

$$h_c = \frac{\bar{q}_c}{A\Delta T} = \left(\frac{3}{4}\frac{\nu^2}{k^3 g}\right)^{-\frac{1}{3}} Re_o^{-\frac{1}{3}}\,\psi_1\left(B_o, \frac{D_o}{L-L_d}, Re_o, Re_L\right) \tag{A9}$$

where

$$\psi_1 = \left(\frac{Re_o}{Re_L}\right)^{\frac{1}{3}} + \frac{D_o}{B_o^4(L - L_d)} Re_o^{\frac{1}{3}}\left\{\frac{2}{3}B_o^3\left(Re_o^{\frac{2}{3}} - Re_L^{\frac{2}{3}}\right) - 2B_o^2\left(Re_o^{\frac{1}{3}} - Re_L^{\frac{1}{3}}\right)\right.$$

$$\left. - \left[\frac{4}{3}\left(1 + B_o Re_o^{\frac{1}{3}}\right)^3 - 6\left(1 + B_o Re_o^{\frac{1}{3}}\right)^2 + 12\left(1 + B_o Re_o^{\frac{1}{3}}\right) - 4\ln\left(1 + B_o Re_o^{\frac{1}{3}}\right)\right.\right.$$

$$+ 4 \ln\left(1 + B_o \, Re_L^{\frac{1}{3}}\right) - \frac{22}{3}\Bigg]\left(Re_L^{-\frac{1}{3}} - Re_o^{-\frac{1}{3}}\right) + 4\left(B_o + Re_o^{-\frac{1}{3}}\right)\left[\ln\left(1 + B_o \, Re_o^{\frac{1}{3}}\right) - \ln\left(1 + B_o \, Re_L^{\frac{1}{3}}\right)\right]\Bigg\} \tag{A10a}$$

The function ψ_1 will always assume values greater than unity. In equation (A10a), Re_L is the Reynolds number when z=L, which can be calculated numerically from equation (A4).

In the case of no boiling (i.e., B_o=o), ψ_1 has the following simpler form which can be obtained by integrating equation (A1) with q_b=o:

$$\psi_1 = \frac{4}{3}\frac{D_o}{L} Re_o^{\frac{4}{3}}\left\{1 - \left(1 - \frac{L}{D_o} Re_o^{-\frac{4}{3}}\right)^{\frac{3}{4}}\right\} \tag{A10b}$$

When $L = D_o \, Re_o^{4/3}$, dryout occurs and ψ_1 has a maximum value of 4/3 (or 1.33).

A.2.2 Formulation Using the Chun-Seban Correlation

Due to capillary waves, the effective film thickness for heat conduction is somewhat less than the Nusselt value, which accounts for an increase in heat transfer. Based on the work of Zazuli, Chun and Seban [6], the Nusselt thickness, δ, is related to the effective film thickness δ^*, as follows:

$$\frac{\delta^*}{\delta} = \frac{4}{3}\left(\frac{4\Gamma}{\mu}\right)^{-\frac{1}{9}} \tag{A11}$$

provided the following conditions are both true:

$$\frac{4\Gamma}{\mu} \geq 2.43\left(\frac{\mu^4 g}{\rho\,\sigma}\right)^{-\frac{1}{11}} \tag{A12}$$

and

$$\frac{4\Gamma}{\mu} \geq 13.4 \tag{A13}$$

If either condition is not satisfied, then capillary waves are not present and $\delta^*/\delta = 1$ (i.e., the analysis of the previous section is applicable). When conditions (A12) and (A13) are satisfied, the Chun-Seban correlation is employed:

$$\frac{q_c}{A} = k\frac{\Delta T}{\delta^*} = k\,\Delta T\,\frac{3}{4}\left(\frac{3}{4}\frac{\nu^2}{g}\right)^{-\frac{1}{3}}\left(\frac{4\Gamma}{\mu}\right)^{-\frac{2}{9}} \tag{A14}$$

In the text the Chun-Seban correlation was expressed in an alternate form in terms of h_c, where $h_c = (q_c/A)/\Delta T$, see equation (8d). With q_c/A expressed as equation (A14), equation (A1) can be integrated subject to the boundary

condition that $\Gamma = \Gamma_o$ at $z = L_d$ to yield:

$$\frac{1}{9} b_o^5 \left(Re_o - Re\right) - \frac{1}{7} b_o^4 \left(Re_o^{\frac{7}{9}} - Re^{\frac{7}{9}}\right) + \frac{1}{5} b_o^3 \left(Re_o^{\frac{5}{9}} - Re^{\frac{5}{9}}\right)$$
$$- \frac{1}{3} b_o^2 \left(Re_o^{\frac{1}{3}} - Re^{\frac{1}{3}}\right) + b_o \left(Re_o^{\frac{1}{9}} - Re^{\frac{1}{9}}\right) - \sqrt{b_o}\left[\tan^{-1}\left(\sqrt{b_o}\, Re_o^{\frac{1}{9}}\right) - \tan^{-1}\left(\sqrt{b_o}\, Re^{\frac{1}{9}}\right)\right]$$
$$= \frac{b_o^6}{16} \frac{(z-L_d)}{D_o} \tag{A15}$$

In equation (A15),

$$b_o = \frac{4}{3} B_o \tag{A16}$$

where B_o is defined in equation (A6). The average of q_c/A over $L_d \le z \le L$ is:

$$\frac{\bar{q}_c}{A} = \frac{1}{(L-L_d)} \int_{L_d}^{L} \frac{q_c}{A}\, dz \tag{A17}$$

which, upon integration, yields the average heat transfer coefficient:

$$h_c = \frac{\bar{q}_c}{A\Delta T} = \frac{3}{4} \left(\frac{3}{4} \frac{\nu^2}{k^3 g}\right)^{-\frac{1}{3}} Re_o^{-\frac{2}{9}}\, \psi_2 \left(b_o, \frac{D_o}{L-L_d}, Re_o, Re_L\right) \tag{A18}$$

where

$$\psi_2 = \left(\frac{Re_o}{Re_L}\right)^{\frac{2}{9}} + \frac{16}{b_o^6} \frac{D_o}{(L-L_d)} Re_o^{\frac{2}{9}} \left\{\frac{2}{63} b_o^5 \left(Re_o^{\frac{7}{9}} - Re_L^{\frac{7}{9}}\right) - \frac{2}{35} b_o^4 \left(Re_o^{\frac{5}{9}} - Re_L^{\frac{5}{9}}\right)\right. \tag{A19}$$
$$+ \frac{2}{15} b_o^3 \left(Re_o^{\frac{1}{3}} - Re_L^{\frac{1}{3}}\right) - \frac{2}{3} b_o^2 \left(Re_o^{\frac{1}{9}} - Re_L^{\frac{1}{9}}\right) + b_o \left(Re_L^{-\frac{1}{9}} - Re_o^{-\frac{1}{9}}\right)$$
$$- \left[\frac{1}{9} b_o^5 Re_o^3 - \frac{1}{7} b_o^4 Re_o^{\frac{7}{9}} + \frac{1}{5} b_o^3 Re_o^{\frac{5}{9}} - \frac{1}{3} b_o^2 Re_o^{\frac{1}{3}} + b_o Re_o^{\frac{1}{9}} - \sqrt{b_o} \tan^{-1}\left(\sqrt{b_o}\, Re_o^{\frac{1}{9}}\right)\right.$$
$$\left. + \sqrt{b_o} \tan^{-1}\left(\sqrt{b_o}\, Re_L^{\frac{1}{9}}\right)\right] \left(Re_L^{-\frac{2}{9}} - Re_o^{-\frac{2}{9}}\right)$$
$$\left. + \left(b_o + Re_o^{-\frac{2}{9}}\right)\sqrt{b_o}\left[\tan^{-1}\left(\sqrt{b_o} Re_o^{\frac{1}{9}}\right) - \tan^{-1}\left(\sqrt{b_o}\, Re_L^{\frac{1}{9}}\right)\right]\right\} \tag{A19a}$$

The function ψ_2 will always assume values greater than unity. In equation (A19a), Re_L is the Reynolds number when $z = L$, which can be calculated numerically from equation (A15).

In the case of no boiling (i.e., $b_o = o$), ψ_2 has the following simpler form which can be obtained by integrating equation (A1) with $q_b = 0$:

$$\psi_2 = \frac{16}{9}\ \frac{Do}{L}\ Re_o^{\frac{11}{9}}\left\{1-\left(1-\frac{11}{16}\frac{L}{D_o}\ Re_o^{-\frac{11}{9}}\right)^{\frac{9}{11}}\right\} \tag{A19b}$$

When $L = (16/11)\ D_o\ Re_o^{11/9}$, dryout occurs and ψ_2 has a maximum value of 11/9 (or 1.22).

In the event capillary waves are present in only a portion of the film, the overall heat flux can be obtained by calculating separately the contributions in the regions with and without capillary waves, and then averaging the two. For this case, the average heat transfer coefficient is given as:

$$h_c = \frac{3}{4}\left(\frac{3}{4}\ \frac{\nu^2}{k^3 g}\right)^{-\frac{1}{3}} Re_o^{-\frac{2}{9}}\ \psi_2\left(b_o, \frac{D_o}{L_c - L_d}, Re_o, Re_c\right)\ \frac{(L_c - L_d)}{(L - L_d)}$$

$$+\left(\frac{3}{4}\ \frac{\nu^2}{k^3 g}\right)^{-\frac{1}{3}} Re_o^{-\frac{1}{3}}\ \psi_1\left(B_\sigma, \frac{D_o}{L-L_c}, Re_c, Re_L\right)\left(\frac{L-L_c}{L-L_d}\right) \tag{A20}$$

where Re_c is the critical Reynolds number below which capillary waves are not present and L_c is the value of z when the Reynolds number is Re_c. The critical Reynolds number can be obtained from equations (A12) and (A13) and the value of L_c can be obtained from equation (A15).

A2. Turbulent Case

For the turbulent case an energy balance yields a differential equation identical to equation (A1):

$$\frac{q_b}{A} + \frac{q_c}{A} = -\frac{d\Gamma}{dz}\ h'_{fg} \tag{A1}$$

but here the expression for q_c/A is given by the turbulent form of the Chun-Seban correlation:

$$\frac{q_c}{A\Delta T} = 3.8 \times 10^{-3}\left(\frac{\nu}{\alpha}\right)^{0.65}\left(\frac{\nu^2}{k^3 g}\right)^{-\frac{1}{3}}\left(\frac{4\Gamma}{\mu}\right)^{\frac{2}{5}} \tag{A21}$$

which is equation (8e) in the text.

Substituting equation (A21) into equation (A1) gives a first order differential equation which can be integrated subject to the boundary condition $\Gamma = \Gamma_o$ at $z = L_d$ to yield.

$$\frac{1}{3}\left(Re_o^{3/5} - Re^{3/5}\right) - \frac{B_o}{a}\left(Re_o^{1/5} - Re^{1/5}\right) + \left(\frac{B_o}{a}\right)^{3/2}$$

$$\left[\tan^{-1}\left(\sqrt{\frac{a}{B_o}}\ Re_o^{1/5}\right) - \tan^{-1}\left(\sqrt{\frac{a}{B_o}}\ Re^{1/5}\right)\right] = \frac{3a}{20}\ \frac{(z-L_d)}{D_o} \tag{A22}$$

where

$$a = 3.8 \times 10^{-3} \left(\frac{3}{4}\right)^{\frac{1}{3}} \left(\frac{\nu}{\alpha}\right)^{0.65} \tag{A23}$$

and Re, Re_o, B_o, D_o are defined previously in equations (A5), (A6), and (A7).

The average of q_c/A over $L_d \leq z \leq L$ is

$$\frac{\bar{q}_c}{A} = \frac{1}{L-L_d} \int_{L_d}^{L} \frac{q_c}{A} \, dz \tag{A24}$$

With equations (A1) and (A22), equation (24) can be integrated to yield the average heat transfer coefficient:

$$h_c = a\left(\frac{3}{4} \frac{\nu^2}{k^3 g}\right)^{-\frac{1}{3}} Re_o^{\frac{2}{5}} \phi_1 \tag{A25}$$

with

$$\begin{aligned}
\phi_1 = &\left(\frac{Re_L}{Re_o}\right)^{2/5} + \frac{20}{3a} \frac{D_o}{(L-L_d)} Re_o^{-2/5} \left\{ \frac{2}{15}\left(Re_L - Re_o\right) - \frac{2B_o}{3a}\left(Re_L^{3/5} - Re_o^{3/5}\right) \right. \\
&+ \left(\frac{B_o}{a}\right)^{3/2} \left[\left(Re_L^{2/5} + \frac{B_o}{a}\right) \tan^{-1}\left(\sqrt{\frac{a}{B_o}} Re_L^{1/5}\right) - \sqrt{\frac{B_o}{a}} Re_L^{1/5} \right] \\
&- \left(\frac{B_o}{a}\right)^{3/2} \left[\left(Re_o^{2/5} + \frac{B_o}{a}\right) \tan^{-1}\left(\sqrt{\frac{a}{B_o}} Re_o^{1/5}\right) - \sqrt{\frac{B_o}{a}} Re_o^{1/5} \right] \\
&\left. - \left[\frac{1}{3} Re_o^{3/5} - \frac{B_o}{a} Re_o^{1/5} + \left(\frac{B_o}{a}\right)^{3/2} \tan^{-1}\left(\sqrt{\frac{a}{B_o}} Re_o^{1/5}\right) \right] \left(Re_L^{2/5} - Re_o^{2/5}\right) \right\}
\end{aligned} \tag{A26a}$$

The function ϕ_1 will always assume values less than unity. In equation (A26a) Re_L is the Reynolds number when z=L, which can be numerically obtained from equation (A22).

In the case of no boiling (i.e., B_o=o), ϕ_1 has the following simpler form which can be obtained by integrating equation (A1) with q_b=o:

$$\phi_1 = \frac{4}{3}\frac{D_o}{aL}\,Re_o^{\frac{3}{5}}\left\{1-\left(1-\frac{9}{20}\frac{aL}{D_o}\,Re_o^{-\frac{3}{5}}\right)^{\frac{5}{3}}\right\} \qquad \text{(A26b)}$$

When $L = (20/9)(D_o/a)\,Re_o^{3/5}$, dryout occurs and ϕ_1 has a minimum value of 3/5.

A.3 Comparison of Simple Model and Differential Formulation

The simple model consists of equation (8) with h_c given by equation (8d) for laminar films and equation (8e) for turbulent films. In the more exact differential formulation the value of h_c is given by equation (A18) or (A20) for laminar films and equation (A25) for turbulent films.

Figure A-1 gives a comparison of the exact and simple models as applied to the case of water on a single horizontal tube, with and without boiling. The largest variance between the simple and exact models occurs near dryout. On a percentage basis the maximum deviation at dryout is observed for the case of no boiling and amounts to about 23%. (For cases where capillary waves are present over the entire fully developed region, and if $h_b = 0$ and $L_d/L \to 0$, equation (A19b) shows that the maximum possible variance is 22%. For cases where capillary waves are completely absent, equation (A10b) shows that the maximum variance is 33%. This latter situation is encountered only when the feed flow is unsually low and represents a rather unimportant case.) In laminar flow, film-thinning tends to increase the heat transfer coefficient relative to a film of constant thickness. Thus the exact model, which accounts for film-thinning, exhibits a higher $\bar{h}$ than the simple model, which assumes a constant thickness. Furthermore, since $\bar{h}$ is higher for the exact model, the flowrate at dryout is somewhat greater. Comparisions for ammonia, given in Figure A-2, demonstrate the same general behavior observed with water. In Figures A-1 and A-2, it can be seen that the exact and simple models quickly merge at about $\Gamma = 0.01$ kg/s-m. Although not shown, the models remain coincident throughout the entire laminar ranges; i.e., to $\Gamma = 0.232$ kg/s-m (Re = 3170) for water and to $\Gamma = 0.148$ kg/s-m (Re = 2660) for ammonia. Thus except near dryout the simple model affords a good approximation of the exact model for laminar films on single tubes.

In the text it was indicated that the Chun-Seban correlation provides an indication of the lower limit of heat transfer for a bank of plain tubes. (With boiling enhancement the lower limit is Chun-Seban + h_b.) The Chun-Seban correlation based on constant flowrate essentially constitutes the simple model. The differential formulation also incorporates the Chun-Seban correlation but accounts for the change in Γ with z. As with single tubes it was found that the largest variance between the exact and simple models occurs at dryout, and in the worst case the exact model overpredicts the simple model by 22%. The variance between the models decreases until the transition Reynolds number is reached. Thereafter the models slightly diverge, but now the simple model overpredicts the exact model. This is a consequence of the fact that in the turbulent regime, the local value of h_c

decreases with flowrate, see equation (8e). Accordingly the simple model, which assumes a constant flowrate, will predict a higher heat transfer coefficient than the exact model, which accounts for the decreasing flowrate. Except for certain limiting cases the simple model generally provides a good approximation to the more exact differential formulation for both the laminar and turbulent ranges.

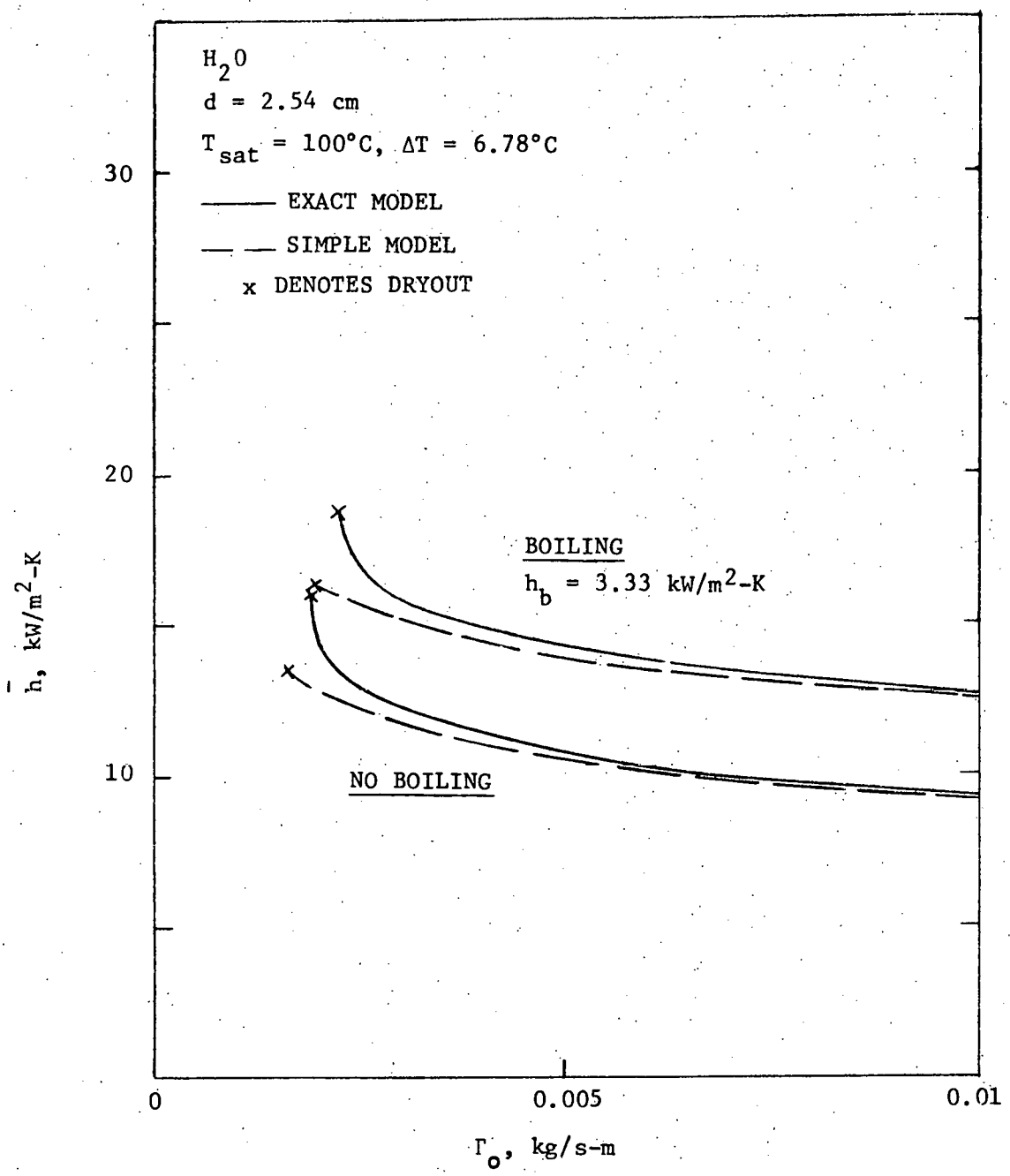

FIGURE A-1. COMPARISON OF EXACT AND SIMPLE MODEL FOR WATER.

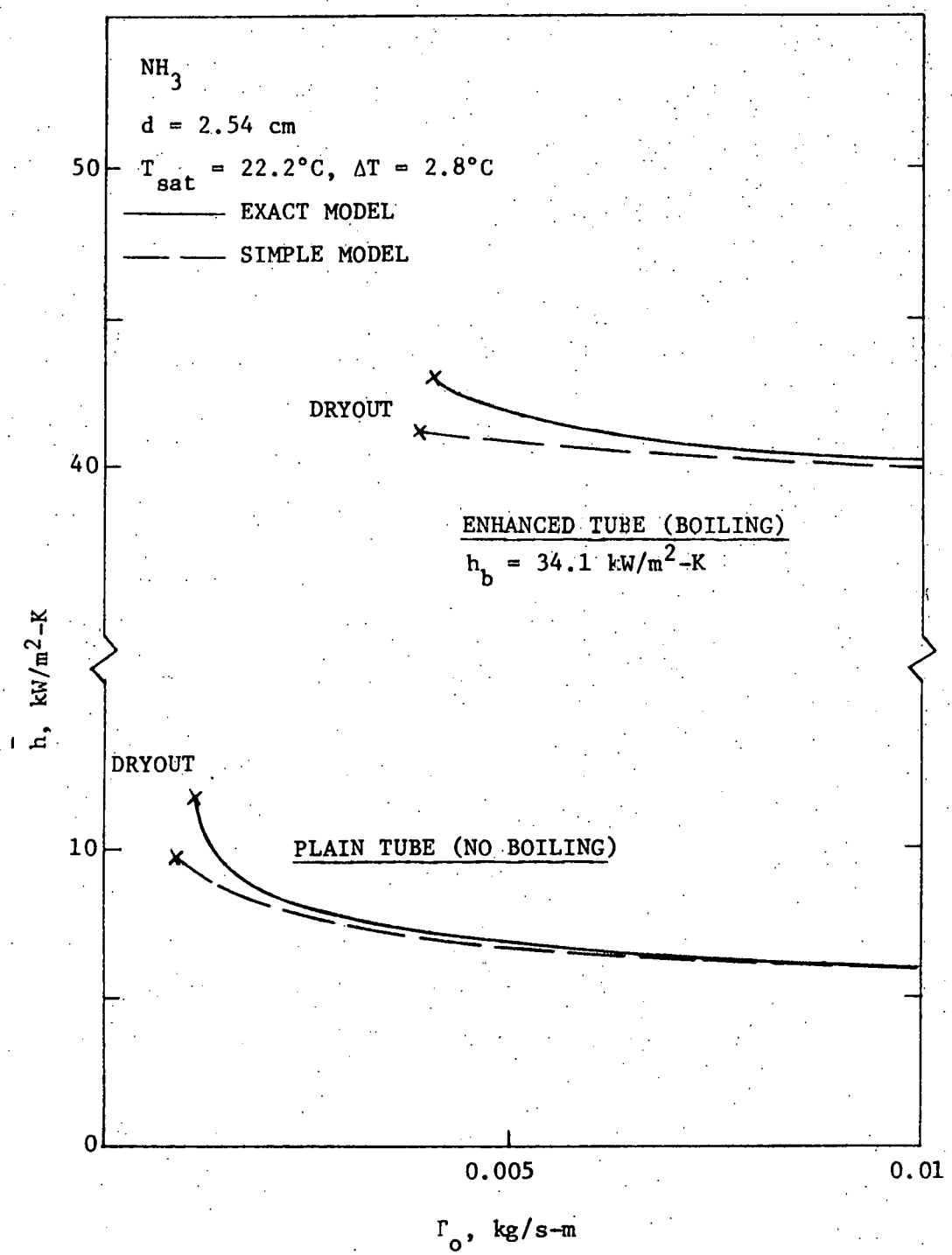

FIGURE A-2. COMPARISON OF EXACT AND SIMPLE MODEL FOR AMMONIA.